J Nanopart Res (2013) 15:1985
DOI 10.1007/s11051-013-1985-7

RESEARCH PAPER

Surfactant-assisted dispersion of carbon nanotubes: mechanism of stabilization and biocompatibility of the surfactant

Raman Preet Singh · Sanyog Jain · Poduri Ramarao

Received: 19 April 2013 / Accepted: 28 August 2013 / Published online: 12 September 2013

Abstract Nanoparticles (NPs) are thermodynamically unstable system and tend to aggregate to reduce free energy. The aggregation property of NPs results in inhomogeneous exposure of cells to NPs resulting in variable cellular responses. Several types of surfactants are used to stabilize NP dispersions and obtain homogenous dispersions. However, the effects of these surfactants, per se, on cellular responses are not completely known. The present study investigated the application of Pluronic F68 (PF68) for obtaining stable dispersion of NPs using carbon nanotubes as model NPs. PF68-stabilized NP suspensions are stable for long durations and do not show signs of aggregation or settling during storage or after autoclaving. The polyethylene oxide blocks in PF68 provide steric hindrance between adjacent NPs leading to stable NP dispersions. Further, PF68 is biocompatible in nature and does not affect integrity of mitochondria, lysosomes, DNA, and nuclei. Also, PF68 neither induce free radical or cytokine production nor does it interfere with cellular uptake mechanisms. The results of the present study suggest that PF68-assisted dispersion of NPs produced suspensions, which are stable after autoclaving. Further, PF68 does not interfere with normal physiological functions suggesting its application in nanomedicine and nanotoxicity evaluation.

Keywords Carbon nanotubes · Dispersion · Surfactant · Toxicity · Biocompatibility

Introduction

Nanoparticles (NPs) have gained immense popularity in nanomedicine and nanodiagnostics in the recent

Electronic supplementary material The online version of this article (doi:10.1007/s11051-013-1985-7) contains supplementary material, which is available to authorized users.

R. P. Singh (✉) · P. Ramarao (✉)
Department of Pharmacology and Toxicology, National Institute of Pharmaceutical Education and Research, S.A.S. Nagar (Mohali) 160 062, Punjab, India
e-mail: ramanpreetsingh@hotmail.com

P. Ramarao
e-mail: ramaraop@yahoo.com

R. P. Singh · S. Jain · P. Ramarao
Centre for Pharmaceutical Nanotechnology, Department of Pharmaceutics, National Institute of Pharmaceutical Education and Research, S.A.S. Nagar (Mohali) 160 062, Punjab, India

Present Address:
R. P. Singh
Evalueserve SEZ (Gurgaon) Pvt. Ltd., Sector-21, Gurgaon 122 001, Haryana, India

Present Address:
P. Ramarao
School of Basic and Applied Sciences, Central University of Punjab, Bathinda 151 001, Punjab, India

past. The small size of NPs offers unique physicochemical properties useful in drug delivery and diagnostics. NPs possess high specific surface area which allows highly efficient drug loading by surface covalent linkage along with the ability to attach targeting and imaging ligands (Thakare et al. 2010). They also show high oral absorption resulting in high bioavailability, higher therapeutic efficacy, reduced toxicity and tissue targeting (Jain et al. 2011a, b). However, the high surface area represents a thermodynamically high energy state of particles and the system tends to reduce its energy by aggregation (Duan et al. 2011). Therefore, a major challenge associated with formulation of aqueous NP dispersions is their tendency to aggregate during storage leading to phase separation or settling of NPs resulting in non-homogenous suspensions. These non-homogenous dispersions seriously affect the biological properties of NPs including bioavailability and toxicity of NPs. The presence of agglomerates has also been demonstrated to exert biological effects distinct from well-dispersed NPs (Raja et al. 2007; Wick et al. 2007). Several approaches have been suggested for obtaining stable dispersion of NPs including the use of solvents, surfactants, surface functionalization, or supramolecular functionalization (Bihari et al. 2008; Ciofani et al. 2009; Crouzier et al. 2008; Porter et al. 2008). However, each of these approaches has limitations. The use of surfactants suffers from the disadvantage of their toxicity, cost and availability (Bihari et al. 2008; Porter et al. 2008), and difficulty in sterilization (e.g., by autoclaving) (Bihari et al. 2008; Elgrabli et al. 2007; Porter et al. 2008). Chemical functionalization and suspending agents have the potential to alter the electronic structure and physicochemical properties of NPs (Gil et al. 2010).

The studies on dispersion of NPs have mainly concentrated on the stability of dispersion without much concern about the effect of suspending agents on normal cell functions. The surfactants reported to be used for dispersion may themselves be toxic (Blanch et al. 2010; Dong et al. 2008) or may alter the toxicity profile of NPs (Vankoningsloo et al. 2010). Further, the use of natural surfactants (Porter et al. 2008) can also interfere with the inflammatory potential of pro-inflammatory agents (Raychaudhuri et al. 2004).

Cellular uptake represents the first step in cell–NP interactions and is mediated through clathrin, caveolin, and/or macropinocytic mechanisms. The intracellular NPs may then interact with organelles and induce stress responses (e.g., free radical production). In addition, NPs may be sorted to various cellular organelles resulting in organelle damage (Asati et al. 2010; Meng et al. 2009). As a consequence of free radical production and organelle damage, mechanisms involved in inflammation and cell death may be activated. Similar mechanisms have been demonstrated in surfactant-induced cellular death (Inacio et al. 2011; Strupp et al. 2000).

The ability of surfactants to influence the biological responses of NPs as well as the overlapping mechanisms of cell death activated by surfactants and NPs necessitates the need for selection of a suitable surfactant to arrive at a reliable conclusion on biocompatibility/toxicity of NPs under investigation. In this communication, we report a biocompatible surfactant system that produced stable NP using carbon nanotubes (CNTs) as model NPs and investigated the effect of surfactant on cellular stress and cell uptake mechanisms commonly involved in biological effects of NPs. The surfactant neither stimulated stress responses nor interfered with common cell uptake mechanisms involved in NP uptake.

Experimental

Chemicals

Pristine single-walled (SWCNTs) and multi-walled (MWCNTs) CNTs were a gift from Nanovatec, India. Pristine and carboxyl-functionalized (COOH-SWCNT and COOH-MWCNT) CNTs were purchased from AlphaNano Technology Co., Ltd., China. Amine-functionalized SWCNTs were purchased from NanoCarbLab, Russia. Pluronic F68 (PF68) was obtained from Sigma, USA. The source of all other chemicals is provided in electronic supplementary material.

Cells

RAW 264.7, J774.1, A549, A498, Hep G2, and Neuro 2A cell lines were purchased from National Centre for Cell Sciences, Pune, India and maintained in Dulbecco's modified Eagle's medium (DMEM) supplemented with 10 % fetal bovine serum (FBS) as described earlier (Singh and Ramarao 2012). The

final concentration of PF68 and other test substances incubated with cells were prepared in DMEM containing 10 % FBS until otherwise mentioned.

Preparation of NP suspension

PF68 was dissolved in phosphate-buffered saline (PBS; pH 7.4) to obtain 3 % w/v solution. PF68 solution (1 ml) was added to CNT powder (1 mg) and sonicated (UP200S, Hielscher Ultrasonics GmbH, Germany) for 5 min. This CNT stock (CNT 1 mg/ml, PF68 3 % w/v) was used for further studies.

Stability of NP suspensions

CNT stock was diluted tenfold with PBS and kept undisturbed for 3 days. The stability of CNT suspensions was determined by dynamic light scattering (DLS), UV–Vis spectroscopy, and scanning electron microscopy (SEM) as described in electronic supplementary material.

Self-assembly of PF68 on CNTs

The self-assembly of PF68 on CNTs was determined by a novel fluorescence resonance energy transfer (FRET)-based method and nuclear magnetic resonance (NMR).

FRET studies

FRET was performed in aqueous and non-aqueous (phase inversion) medium at 0.3 % PF68 and 0.1 % CNT concentration.

For FRET in aqueous medium, 5-(4,6-dichlorotriazinyl) aminofluorescein (DTAF)-labeled PF68 (DTAF-PF68) was dissolved in water and mixed with rhodamine B isothiocyanate (RBITC)-labeled SWCNT (RBITC–SWCNT) suspension. A drop of suspension was placed on a glass slide and observed under Olympus FV1000 confocal microscope.

For FRET after phase inversion, a drop of aqueous RBITC–SWCNT suspension was smeared on a clean glass slide. The excess water was removed by blotting with a filter paper. A drop of DTAF-PF68 (dissolved in chloroform) was placed on the RBITC–SWCNT smear and observed under confocal microscope. This resulted in a lower aqueous layer and an upper non-aqueous layer.

NMR studies

PF68 was dissolved in D_2O and varying amounts of CNTs were added. The final concentration of PF68 was 1 % w/v while CNT concentrations were 100, 500, and 1000 μg/ml. ^{1}H NMR spectra were obtained on Bruker 300 MHz spectrometer and data were analyzed by TopSpin (Bruker, USA) or MestReNova (Mestrelab, Spain).

Reversibility of PF68 binding to CNTs

DTAF-PF68-dispersed CNT stock suspension was prepared as described in "Experimental" section (preparation of NP suspension) using mild sonication (1 min). CNT stock suspension was diluted tenfold in DMEM or in DMEM containing 10 % FBS, 1 % unlabeled PF68, 0.1 mg/ml Alexa Fluor 647 (AF647)-labeled bovine serum albumin (AF647-BSA), or 1 mg/ml AF647-BSA. CNTs were incubated for 30 min and CNT aggregates were viewed under confocal microscope.

Cell viability and culture medium characteristics

Cells (RAW 264.7, J774.1, A549, A498, Hep G2, and Neuro 2A) were incubated with indicated concentrations of PF68 for up to 3 days. The culture medium was removed and cell viability was determined by MTT assay as described earlier (Singh et al. 2012; Singh and Ramarao 2012). Changes in culture medium characteristics (pH and osmolarity) following addition of PF68 were determined. Cells were incubated with culture medium in presence or absence of 0.3 % PF68. The pH and osmolarity of culture medium were determined on day 0 and day 3. The osmolarity was determined using Vapro 5520 system (Wescor, Inc., USA).

Cell–CNT interactions

Confluent cultures of RAW 264.7 cells were harvested by trypsinization and cell density was adjusted to 10,000 cells/ml. The cell suspension (200 μl/well) was added in each well of a 96-well culture plate and cells were allowed to adhere overnight. The culture medium was removed and replaced with fresh medium containing 100 μg/ml CNTs dispersed in 0.3 % w/v PF68 or PBS. After 3 days of incubation, wells were scanned before and after washing thrice with PBS. In

addition, RAW 264.7 cells were incubated with DTAF-labeled CNTs (dispersed in PF68 or PBS) for 3 days. Cellular uptake of fluorescent CNTs was determined by flow cytometry using BD FACScan (BD Biosciences, USA).

Assay of cellular physiological functions

RAW 264.7 cells were seeded in 96-well plates and incubated with 0.3 % PF68 or positive control for 24 h unless otherwise mentioned. The culture supernatants were collected, cells washed with PBS, and assays performed as described below.

The effect of PF68 on cell size and intracellular complexity; induction of apoptosis; free radical and cytokine generation; cell membrane, mitochondria, lysosomal, nuclear and DNA integrity; and cellular uptake mechanisms was determined as described in electronic supplementary material.

Statistical analysis

All values are expressed as mean ± SEM. Treatment groups were compared by one-way ANOVA followed by Tukey's test.

Results

Cell viability and culture medium characteristics

Cell viability assay of RAW 264.7 cells incubated with PF68 showed that cell viability remained unaffected by PF68 up to a concentration of 0.3 %

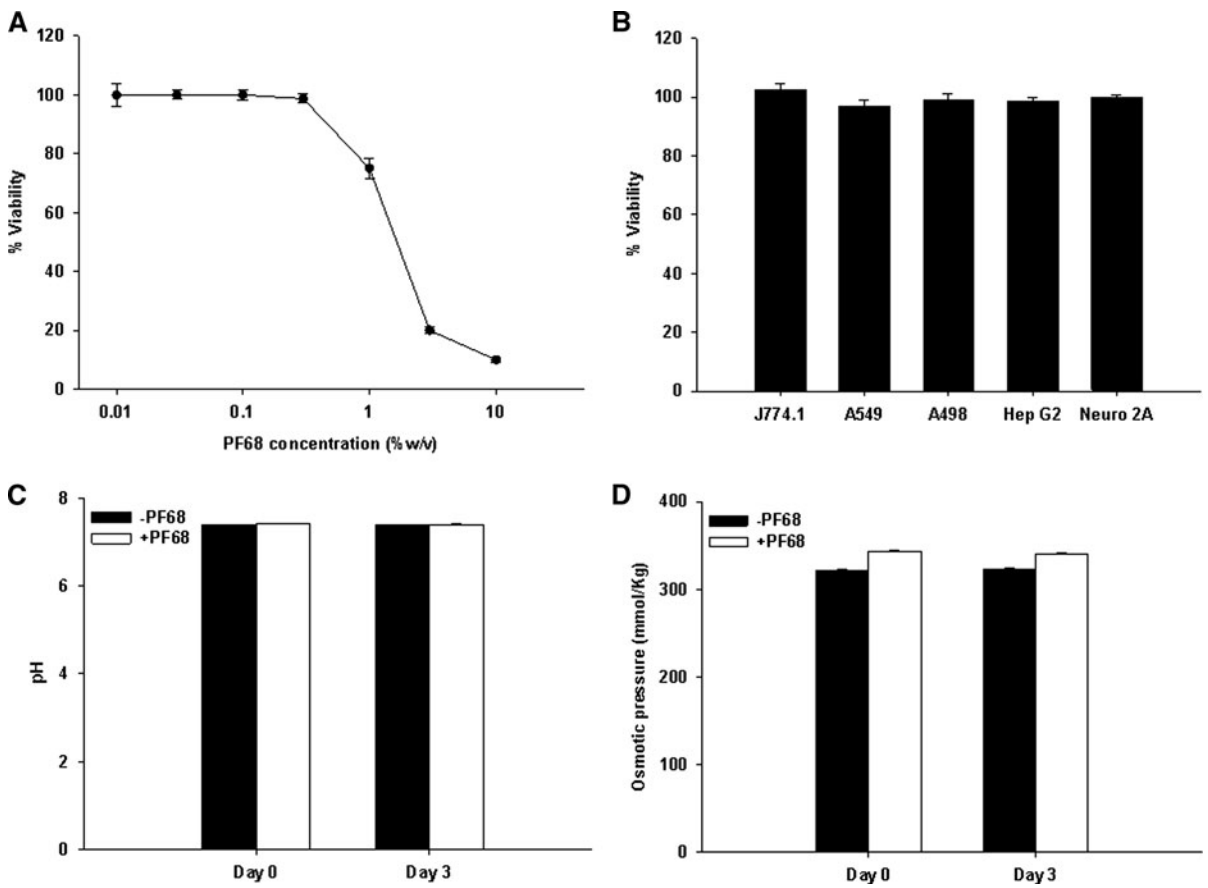

Fig. 1 **a** RAW 264.7 cells were incubated with various concentrations of PF68 and cell viability was determined after 3 days ($n = 10$/concentration). **b** Cell viability of 5 cell lines determined after 3 days incubation with 0.3 % PF68 ($n = 10$/concentration). pH (**c**) and osmotic pressure (**d**) of culture medium with (+PF68) and without (−PF68) 0.3 % PF68 on day 0 and day 3 ($n = 4$/concentration). Data are expressed as mean ± SEM

(Fig. 1a). Further, 0.3 % PF68 was non-toxic in macrophage (J774.1), pulmonary epithelial (A549), renal epithelial (A498), hepatocyte (Hep G2), and neuronal (Neuro 2A) cell lines also (Fig. 1b). In order to rule out the toxic effects that may arise due to non-specific effects of PF68, we evaluated the effect of addition of PF68 on culture medium pH and osmolarity. It was observed that the pH of medium remained unchanged in presence of PF68 on day 0 and after 3 days of incubation (Fig. 1c). Similarly, the osmolarity of culture medium also remained unchanged in presence of 0.3 % PF68 on day 0 and after 3 days of incubation (Fig. 1d). Hence, 0.3 % PF68 was selected for further studies.

Stability of NP suspensions

The ability of PF68 to stabilize NPs was determined using CNTs as model NPs following autoclaving and storage for 3 days. DLS studies showed that size distribution was similar in unsterile and autoclaved CNT suspensions on day 3. Further, the size distribution in CNT suspensions was similar on day 0 and day 3 suggesting that CNTs remain stably dispersed after 3 days. Representative DLS results of SWCNT and MWCNT are shown in Fig. 2a and b, respectively. The mean hydrodynamic size and size distribution [polydispersity index (PDI)] did not significantly change during the study duration (3 days) (Table 1).

It may be argued that the overlapping size distribution in fresh and stored CNT suspensions may arise due to settling of CNT aggregates while individual CNTs remain dispersed. To rule out this possibility, recovery of CNTs from PF68-dispersed CNT suspensions as well as homogeneity of CNT suspensions was determined by UV–Vis spectroscopy. Spectroscopic analysis showed that >80 % of CNTs remained in suspension after removal of aggregated CNTs by centrifugation. It needs to be mentioned here that the reduction in amount of CNTs calculated after storage or centrifugation is not due to settling of CNT aggregates but due to adsorption of CNTs in glass vials (during 3 days storage) and in plastic microcentrifuge tubes (during centrifugation). The quantitative results of CNT recovery are shown in Table 2. Further, homogeneity analysis showed that CNT content in samples drawn from top, middle, and bottom of CNT suspensions was within 10 % of the theoretical concentrations (data not shown). The results of DLS and UV–Vis spectroscopy were further confirmed by SEM which also showed absence of aggregated CNTs in MWCNT samples after autoclaving and storage for 3 days (Fig. 2c).

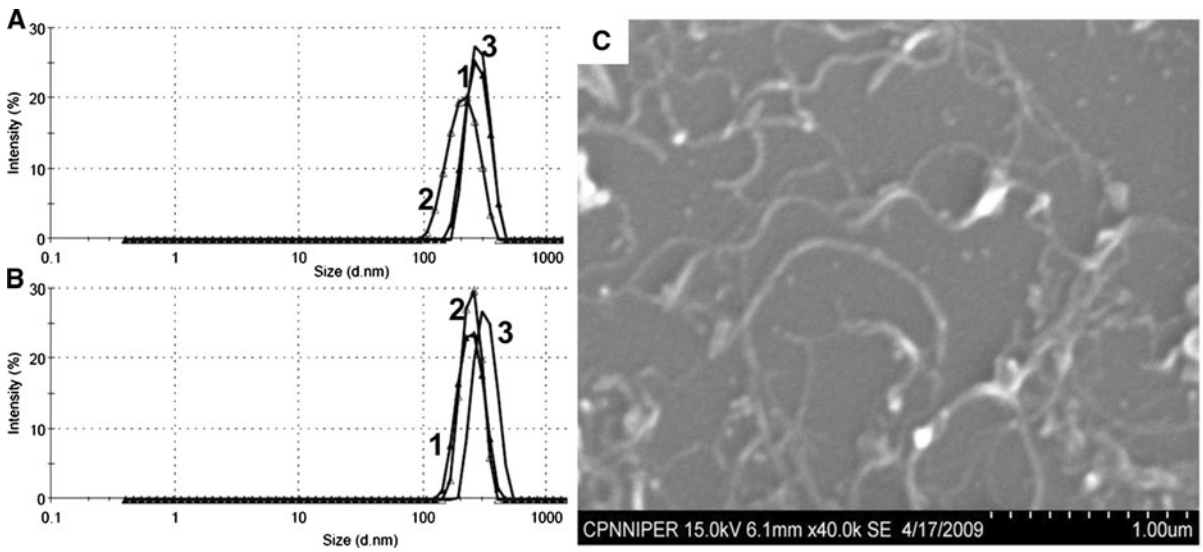

Fig. 2 DLS analysis of SWCNTs **a** and MWCNTs **b** dispersed in 0.3 % PF68. *Filled triangle* (plot 1) and *open triangle* (plot 2) indicate size distribution of non-sterile and autoclaved CNT suspension, respectively, 3 days post-dispersion. The *solid line* (plot 3) shows size distribution on day 0. **c** SEM of autoclaved MWCNT sample shows individual tubes after 3 days post-autoclaving

Table 1 DLS analysis of PF68-dispersed CNTs

CNT type	Supplier	Diameter (nm)[a]	Length (μm)[a]	Day 0		Day 3			
						Unsterile		Sterile	
				Size	PDI	Size	PDI	Size	PDI
SWCNT	Nanovatec, India	1–1.2	~20	358.6 ± 9.0	0.403 ± 0.014	398.9 ± 62.3	0.412 ± 0.050	377.1 ± 43.7	0.436 ± 0.036
MWCNT	Nanovatec, India	20–30	~20	366.8 ± 9.3	0.205 ± 0.061	319.1 ± 9.7	0.375 ± 0.029	418.3 ± 37.6	0.405 ± 0.056

Data are mean ± SEM of quadruplicate samples

[a] Values as provided by the supplier

Self-assembly of PF68 on CNTs

PF68 is a triblock polymer containing polyethylene oxide (PEO) and polypropylene oxide (PPO) blocks and has the chemical formula $(PEO)_{80}$–$(PPO)_{30}$–$(PEO)_{80}$. Therefore, PF68 can possibly interact with NPs through PEO and/or PPO groups and the mechanism of stabilization of NPs by PF68 was investigated by two approaches: FRET and NMR. FRET analysis revealed that, when dispersed in aqueous medium, no significant FRET was observed between fluorescein-rhodamine FRET pair (supplementary Fig. S1) while phase inversion resulted in a significant increase in FRET efficiency (Supplementary Fig. S2).

NMR spectrum of polymer chains is sensitive to changes in hydration and these changes in hydration can be determined from changes in line shape, line width, and chemical shift in ^{1}H NMR. In ^{1}H NMR, the HDO (4.4 ppm), EO $–CH_2–$ (3.7 ppm), PO $–CH_2–$ (3.5 ppm), and PO $–CH_3–$ (1.2 ppm) signals were analyzed. A reduction in peak height, peak broadening, and peak shifts to lower ppm was observed with an increase in SWCNT concentration from 0 to 1,000 μg/ml. This was also associated with peak broadening and downfield shift of PO and EO blocks. However, the SWCNT concentration-dependent changes in NMR spectrum were more pronounced in PO signals as compared to EO signals (Fig. 3a, b).

Reversibility of PF68 binding to CNTs

CNT-bound PF68 was observed as green fluorescence on CNT bundles (supplementary Fig. S3A). The fluorescence was, however, not observed in CNTs incubated in DMEM-containing FBS or unlabeled PF68 (supplementary Fig. S3B and S3C). Similarly, CNT-bound PF68-associated fluorescence was also reduced in presence of AF647-BSA in a concentration-dependent manner (supplementary Fig. S4).

CNT–cell interactions

CNTs dispersed without surfactant showed tendency to aggregate and formed large floating clumps. The scanned images of wells show that, in the absence of surfactant (−PF68), CNTs were non-uniformly dispersed and formed visible aggregates. On the other hand, PF68-dispersed CNTs (+PF68) were uniformly dispersed throughout the well with no evidence of

Table 2 Recovery of PF68-dispersed CNTs with and without autoclaving

CNT type	Supplier[a]	Diameter (nm)[b]	Length (μm)[b]	Unsterile		Sterile	
				Before centrifugation[c]	After centrifugation[c]	Before centrifugation[c]	After centrifugation[c]
SWCNT	1	1.1.2	~20	88.5 ± 1.0	60.7 ± 8.2	89.1 ± 1.0	86.4 ± 7.8
COOH-SWCNT	2	1–2	~10	92.0 ± 10.1	87.7 ± 10.3	80.9 ± 2.1	82.5 ± 23.2
MWCNT	1	20–30	~20	79.2 ± 0.5	72.2 ± 4.7	82.2 ± 0.3	76.8 ± 3.6
MWCNT	2	20–30	0.5–2	72.6 ± 2.3	77.1 ± 4.8	76.7 ± 1.6	76.3 ± 1.9
MWCNT	2	3–10	0.5–2	91.4 ± 8.5	89.1 ± 7.0	92.3 ± 5.7	93.3 ± 2.8
MWCNT	2	20–30	~20	91.7 ± 2.2	90.0 ± 1.0	98.7 ± 1.3	90.9 ± 2.1
MWCNT	2	3–10	~20	93.2 ± 1.2	95.4 ± 12.8	101.6 ± 5.9	93.3 ± 2.4
COOH-MWCNT	2	3–10	~10	111.9 ± 5.5	94.6 ± 5.9	103.5 ± 1.1	99.3 ± 7.2
COOH-MWCNT	2	20–30	~15	111.5 ± 2.1	102.2 ± 2.7	108.7 ± 1.4	101.3 ± 3.0

Data are mean ± SEM of triplicate samples

[a] Supplier 1: Nanovatec, India, Supplier 2: AlphaNano Technology Co., Ltd., China

[b] Values as provided by the supplier

[c] Values represent % recovery

clumps after 3 days of incubation (Fig. 4a). After incubation, the cells were washed with PBS to remove extracellular CNTs. Significantly large amount of CNTs was retained in wells containing PF68-dispersed CNTs as compared to PBS-dispersed CNTs without PF68 indicating that PF68-dispersed CNTs interact strongly with cells (Fig. 4b). The higher cellular interaction of PF68-dispersed was further confirmed using fluorescent-labeled CNTs. Flow cytometric analysis revealed that cell-associated fluorescence was higher in PF68-dispersed SWCNTs (Fig. 4c) and MWCNTs (Fig. 4d) as compared to CNTs dispersed in PBS without PF68.

Assay of cellular physiological functions

The cell size and cellular complexity were determined by monitoring changes in FSC and SSC, respectively. FSC is an indicator of cell size and an increase in FSC indicates increase in cell size. On the other hand, SSC is an indicator of granularity and membrane roughness and an increase in SSC indicates an increase in cellular complexity/granularity. PF68 did not show change in cell size or complexity following 24 h incubation with RAW 264.7 cells. The FSC–SSC flow cytogram of PF68-treated cells was similar to untreated control cells while significant changes in FSC–SSC cytogram were observed in cells treated with triton X-100 (TX100; positive control) (Fig. 5a).

The induction of apoptosis was determined by annexin V staining of cells. Phosphatidylserine (PS) is located on the cytoplasmic side of cell membrane and is externalized during apoptosis. PS has strong affinity for annexin V and apoptotic cells presenting PS on the cell surface can be identified by annexin V staining. The proportion of apoptotic cells was similar in control and PF68-treated cells while a significant increase in proportion of apoptotic cells was observed in PTX-treated cells (Fig. 5b).

The activation of RAW 264.7 macrophages was determined by monitoring stimulation of ROS, RNS, and cytokine production following incubation with PF68. ROS production in RAW 264.7 cells was determined by 2′,7′-dichlorodihydrofluorescein diacetate (H_2DCF-DA) staining. The H_2DCF-DA is a non-fluorescent compound which can cross cell membrane. The DA moiety is cleaved intracellularly to release H_2DCF. The non-fluorescent compound H_2DCF reacts with ROS and leads to generation of fluorescent DCF. The conversion of H_2DCF to DCF is proportional to ROS levels. Hence, DCF fluorescence can be directly correlated with the degree of ROS generation. The fluorescence intensity of DCF was similar in control and PF68-treated cells while PMA-treated cells showed significantly higher intracellular DCF fluorescence (Fig. 6a). Quantitative estimation of DCF fluorescence also showed no significant increase in ROS production following incubation with PF68 as

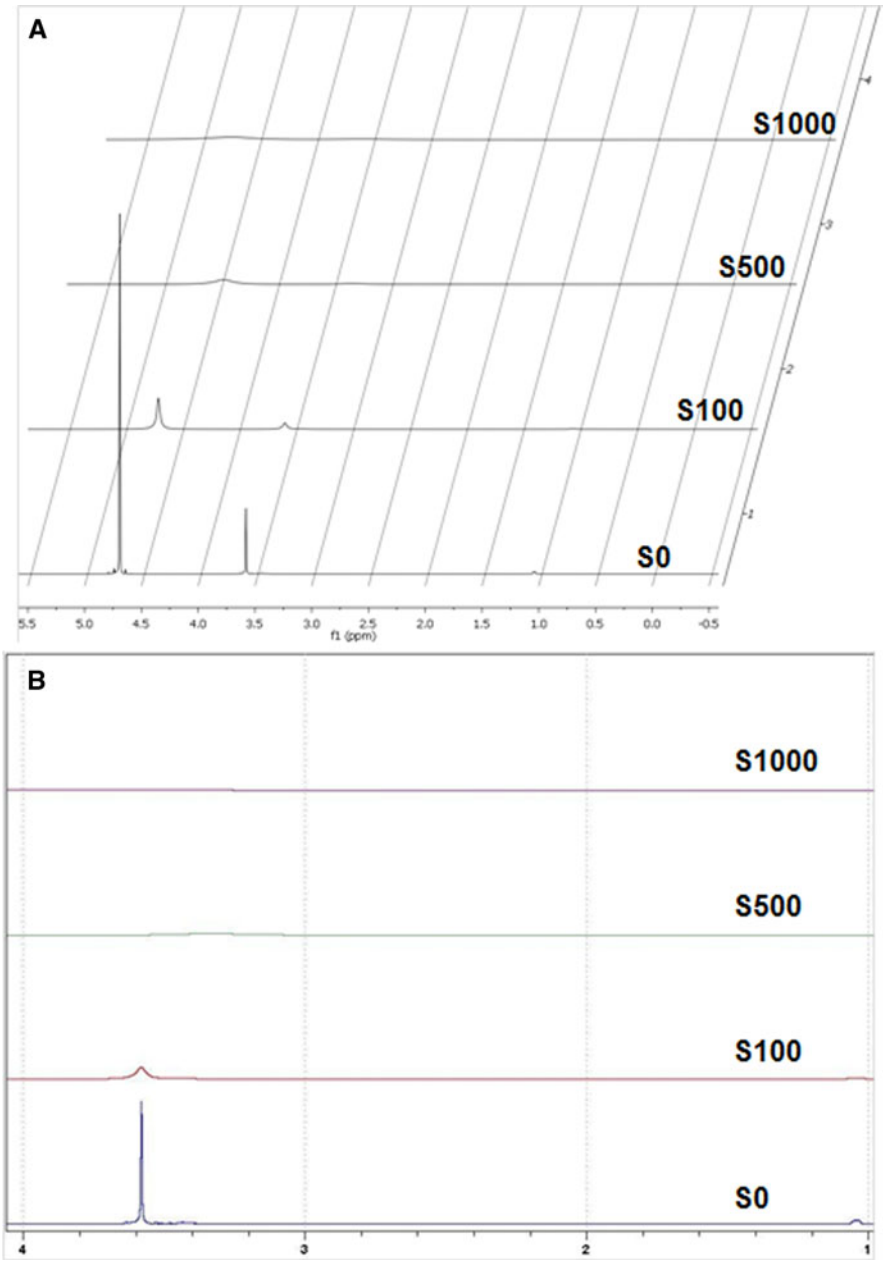

Fig. 3 ^{1}H NMR of PF68 and SWCNTs up to 5.5 (**a**) and 4.0 ppm (**b**). ^{1}H NMR were obtained without (S0) or with 100 (S100), 500 (S500), and 1,000 (S1000) μg/ml of SWCNTs

compared to control cells (Fig. 6b). Similarly, PF68 also did not stimulate RNS and proinflammatory cytokine (tumor necrosis factor-α [TNF-α] and interleukin-6 [IL-6]) production after 24 h incubation with PF68 (Fig. 6b, c).

Cell membrane integrity was determined by propidium iodide (PI) exclusion. PI is a polar molecular and excluded by intact cell membranes. However, when cell membrane is damaged, PI can move inside the cells. Therefore, cells with a damaged cell membrane are fluoresce red while cells with intact cell membrane are non-fluorescent. PI exclusion indicated that <4 % cells had damaged cell membrane in control and PF68-treated wells while >75 % cells stained with PI in TX100-treated cells (Fig. 7a). SEM analysis also revealed that cell membrane integrity remained unaffected following incubation with PF68 while appreciable cell membrane damage was observed in TX100-treated cells (Fig. 7b).

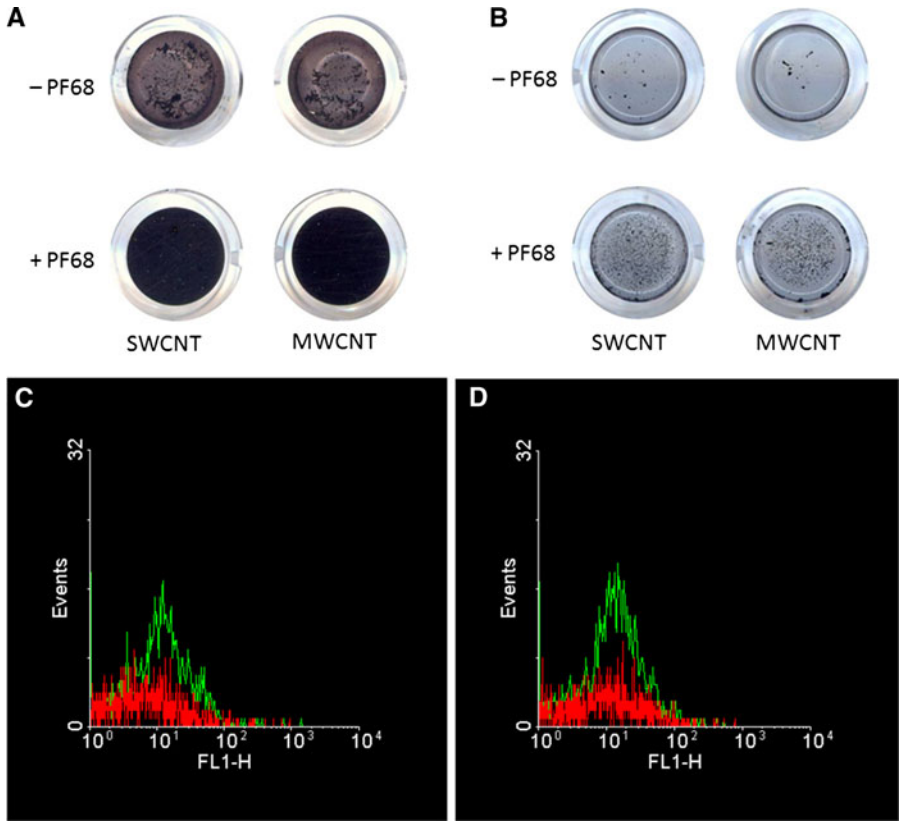

Fig. 4 Scanned wells of a 96-well plate seeded with RAW 264.7 cells containing SWCNTs and MWCNTs with (+PF68) and without (−PF68) PF68 before (**a**) and after (**b**) washing with PBS. Flow cytometric analysis of cellular uptake of fluorescent-labeled SWCNTs (**c**) and MWCNTs (**d**). The *green* and *red* histograms show cellular uptake of CNTs in presence and absence of PF68, respectively. (Color figure online)

Cellular organelle damage was determined by monitoring changes in dye uptake by mitochondria and lysosomes. Cellular uptake of rhodamine 123 (Rh123) was similar in control and PF68-treated cells while dye uptake was reduced in sodium azide treated cells (Fig. 8a). The reduction in Rh123 uptake indicates dissipation of mitochondrial membrane potential (Ψ_m) and mitochondrial damage.

The lysosomal integrity was determined by acridine orange (AO) relocalization. AO is a lysomotropic and metachromatic dye which accumulates in lysosomes. The lysosomal AO gives a red fluorescence. However, when lysosomes are damaged, AO relocalizes to cytoplasm where it gives green fluorescence and the increase in green fluorescence is proportional to lysosomal damage. Cells incubated with PF68 showed no significant AO relocalization while positive control showed a significantly higher increase in AO relocalization (Fig. 8b).

The organelle damage was quantified by colorimetric and fluorimetric analysis of dye uptake. The Ψ_m was similar in control and PF68-treated cells as determined by Rh123 and safranin O (SafO) dye uptake (Fig. 8c). Similarly, PF68 did not induce lysosomal damage since the intensity of AO green fluorescence (due to AO relocalization) was similar in control and PF68-treated cells. Further, the lysosomal integrity was also confirmed by NR uptake. NR accumulates in intact lysosomes and a reduction in NR uptake indicates lysosomal damage. NR uptake was similar in control and PF68-treated cells while a reduction in NR was observed in hydrogen peroxide-treated cells (Fig. 8d).

DNA damage was determined by TUNEL and DPA assay. TUNEL assay is based on the principle that the enzyme terminal deoxynucleotidyl transferase repairs DNA strand breaks by addition of nucleotides. The incorporation of fluorescent nucleotides leads to staining of cells with damaged DNA. On the other hand, DPA reacts with DNA and forms a colored product. Breaking of DNA strands to smaller fragments leads to an increase in intensity of the colored product. The addition of PF68 to culture medium did not increase the frequency of DNA strand breaks since number of TUNEL-positive cells was similar in control and PF68-treated cells (Fig. 9a). Quantitative

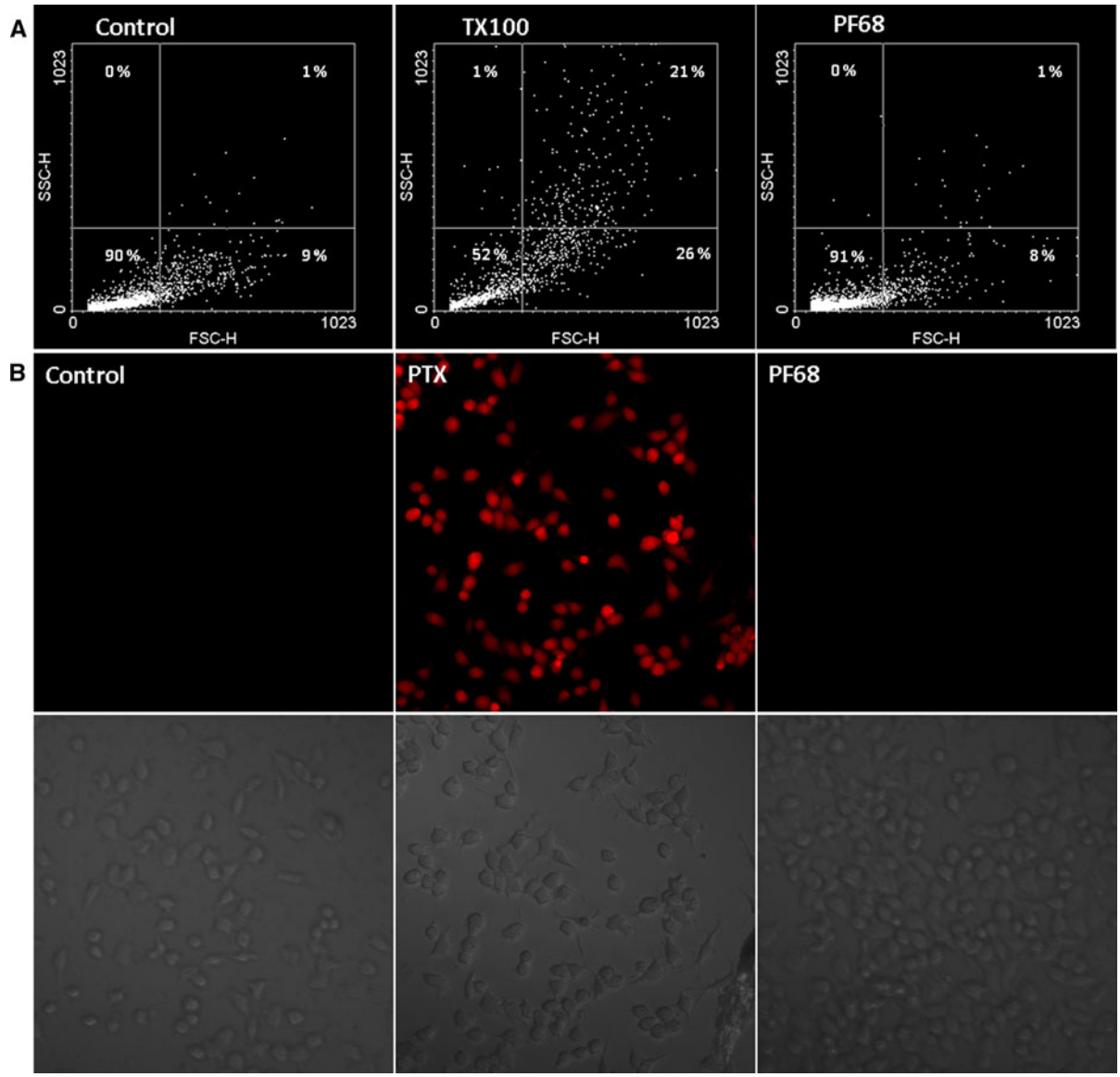

Fig. 5 **a** FSC–SSC correlation cytograms of RAW 264.7 cells incubated with medium alone (control), positive control (TX100), or PF68. **b** Annexin V staining of RAW 264.7 cells incubated with medium alone (control), positive control [paclitaxel (PTX)], or PF68. *Upper panel* in (**b**) shows annexin V-stained cells and lower panel shows DIC images of the same field

analysis also revealed that there was no significant ($P > 0.05$) difference in number of TUNEL-positive cells in control and PF68-treated cells while a significant ($P < 0.001$) increase in TUNEL-positive cells was observed in PTX-treated cells (Fig. 9b). Similarly, DPA assay also showed PF68 did not induce DNA damage after 24 h of incubation (Fig. 9b).

Apart from the effects on DNA, the effect of PF68 on gross nuclear morphology was also determined. PF68 did not induce nuclear condensation or fragmentation in RAW 264.7 cells (Fig. 9c). Quantitative analysis of confocal micrographs showed that the number of cells showing nuclear condensation and fragmentation was similar in control and PF68-treated cells while a significant ($P < 0.001$) increase in

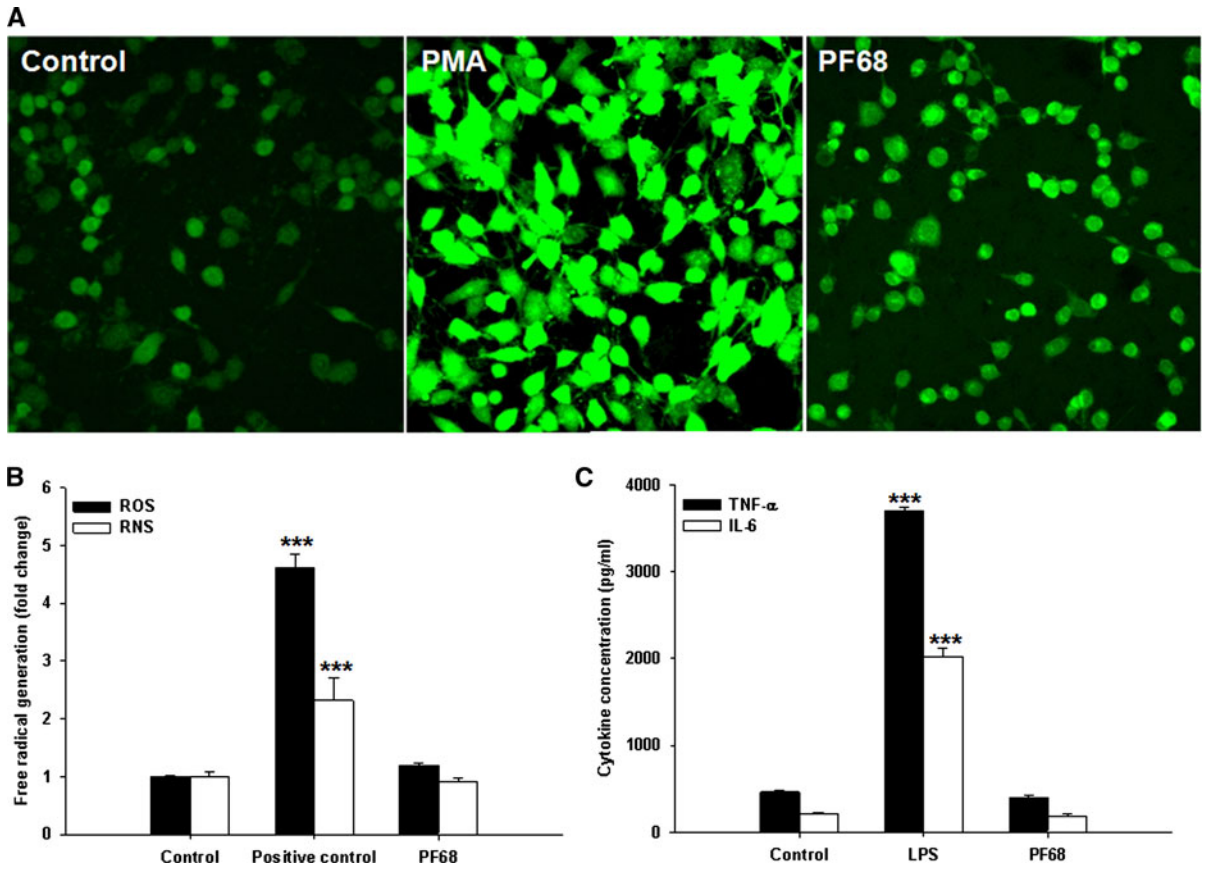

Fig. 6 Free radical (**a**, **b**) and cytokine production (**c**) by RAW 264.7 cells incubated with medium alone (control), positive control [phorbol myristate acetate (PMA) for ROS and lipopolysaccharide (LPS) for RNS and cytokines] or PF68 ($n = 4$–10/concentration). $^{***}P < 0.001$ w.r.t. control determined by One-way ANOVA followed by Tukey's test

nuclear condensation and fragmentation was observed in methotrexate-treated cells (Fig. 9d).

Cellular uptake is mediated by several pathways such as caveolin, clathrin, and fluid phase mechanisms. The effect of PF68 on uptake of fluorescent-labeled markers of caveolin (FITC-BSA), clathrin (FITC-insulin), and fluid phase (FITC-dextran) was determined. PF68 did not alter cellular uptake of caveolin (Fig. 10a), clathrin (Fig. 10b), or fluid phase (Fig. 10c) while specific inhibitors of caveolin, clathrin, and fluid phase transfer inhibited uptake of the markers (Fig. 10).

Discussion

We evaluated several approaches for preparation of stable dispersion of NPs and included use of surfactants, viscosifying agents, solvents, and supramolecular functionalizing agents. CNTs were chosen as model NPs as they represent one of the most challenging NPs with regards to dispersability. The choice of CNTs for PF68-mediated dispersion may be attributed to four major reasons: (1) CNTs have the highest specific area among various types of NPs and therefore represent a thermodynamically unstable system; (2) CNTs are one of the most hydrophobic NPs and aggregation occurs due to hydrophobic and van der Waal's interactions; (3) the high aspect ratio of CNTs also leads to aggregation due to physical entanglement; and (4) the UV–Vis spectral signatures of CNTs and PF68 do not overlap.

Surfactant (PF68)-stabilized NP suspensions were most stable and uniformly dispersed among all the approaches listed above (data not shown). PF68 appeared to be the optimal choice for several reasons.

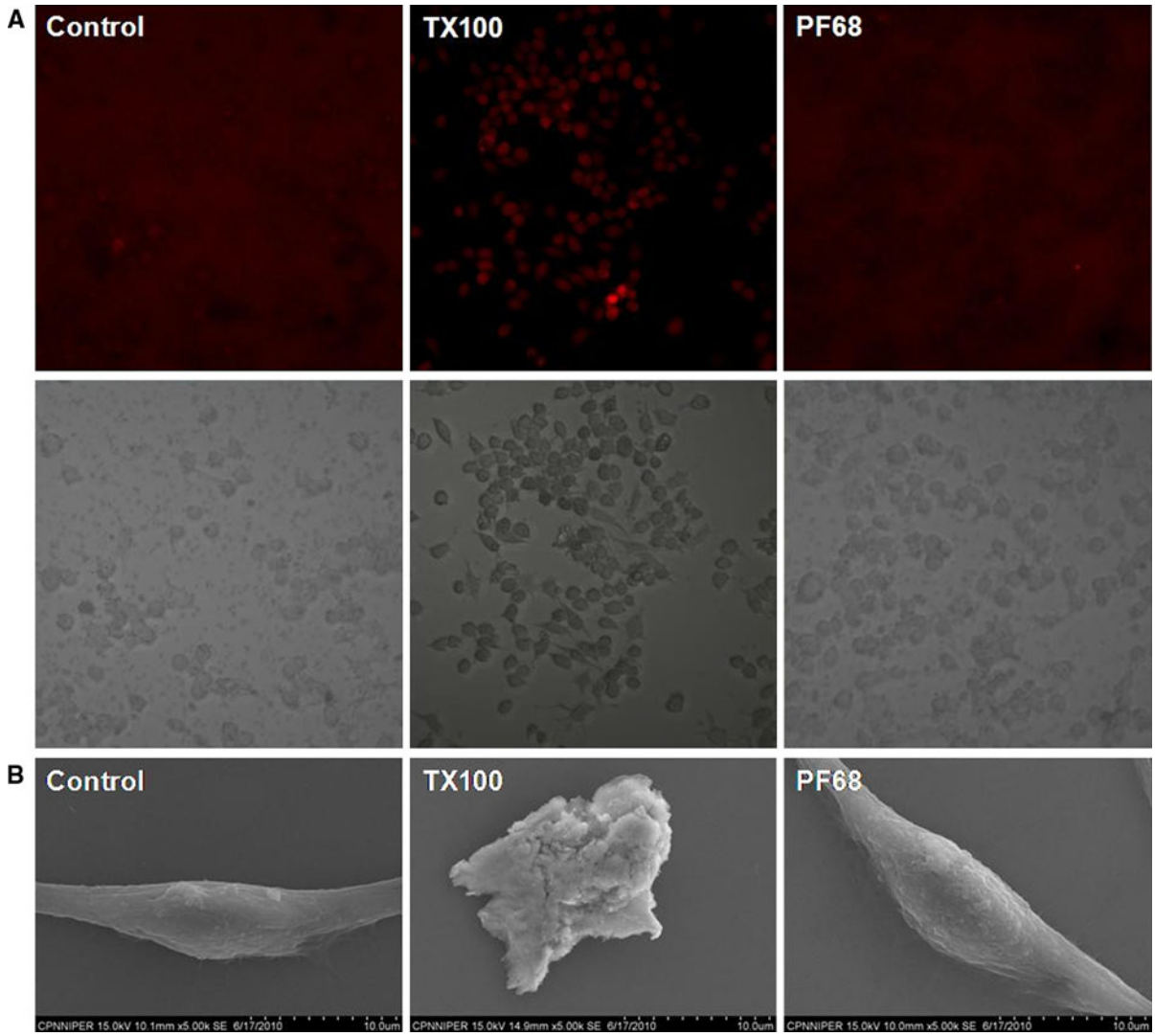

Fig. 7 Cell membrane integrity of RAW 264.7 cells incubated with medium alone (control), positive control (TX100), or PF68 and determined by PI exclusion (**a**) and SEM (**b**). The *upper panel* in (**a**) shows PI-stained cells and lower panel shows DIC images of the same field

First, PF68 is a commonly used pharmaceutical excipient approved by regulatory agencies and can be adopted for NPs intended for human use. We also observed that PF68 did not affect cell viability up to a concentration of 0.3 %. Hence, 0.3 % PF68 was used for stability and biocompatibility studies. Second, PF68-stabilized NPs can be autoclaved without affecting stability of NPs due to its high cloud point (Kabanov and Alakhov 2002). Therefore, PF68 can be used in both sterile and non-sterile formulations without affecting NP stability. Third, pluronics (e.g., PF68) can be used to stabilize a large number of NPs including metallic (Lee et al. 2011), lipidic (Rawat et al. 2011), and polymeric NPs (Ma et al. 2010) apart from CNTs (Antaris et al. 2010).

The mechanism of CNT–PF68 interactions was determined by a novel FRET-based assay and NMR. FRET is a non-radiative energy transfer between two fluorophores and the efficiency of FRET is inversely proportional to the distance between the donor–acceptor FRET pair. We used the fluorescein–rhodamine FRET which has a Forster distance (distance between two fluorophores when FRET efficiency is reduced to 50 %) of 5.6 nm (Kawski et al. 1973).

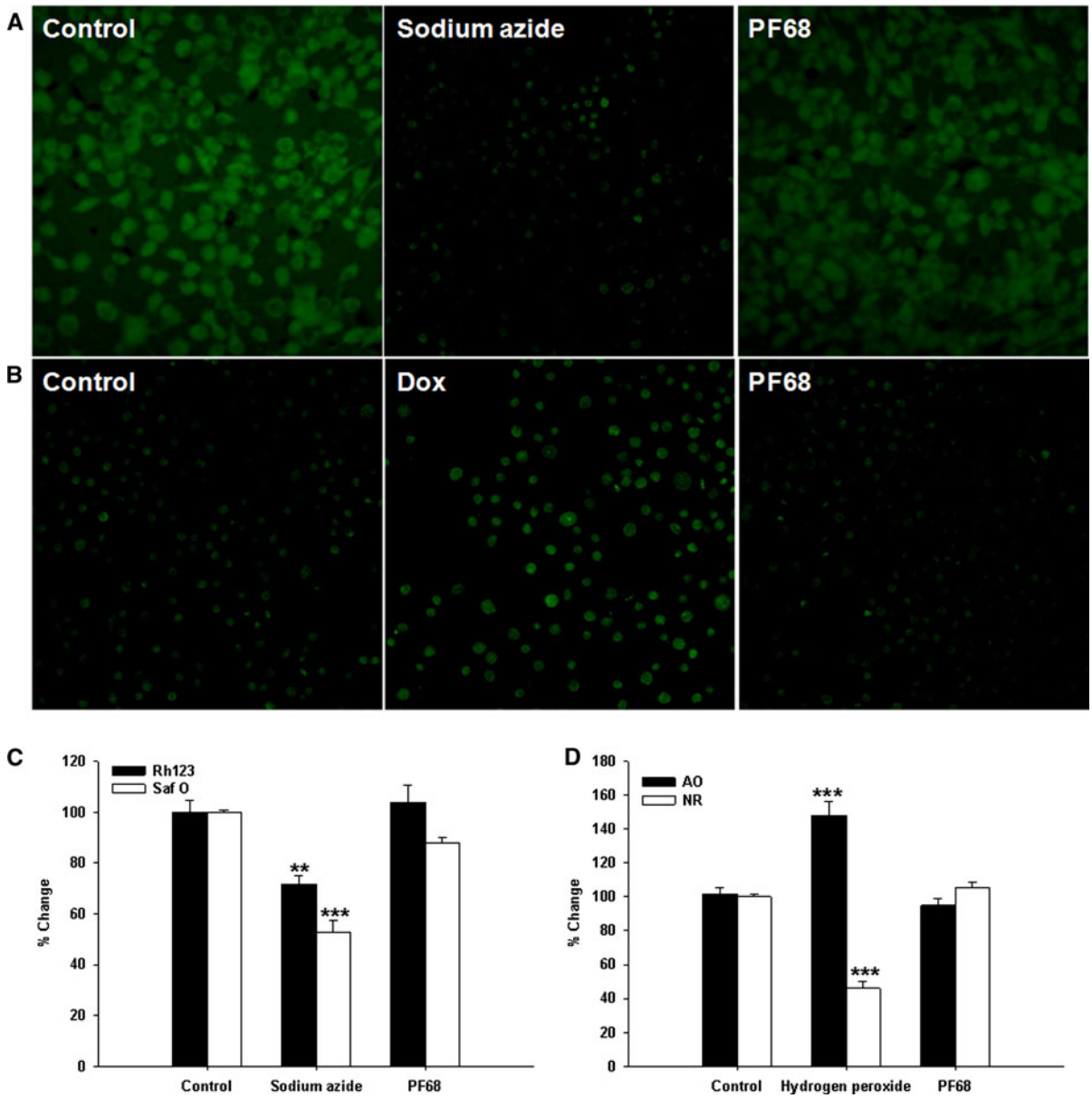

Fig. 8 Mitochondrial and lysosomal integrity of RAW 264.7 cells incubated with medium alone (control), positive control, or PF68 and determined by Rh123 staining (**a**) and AO relocalization (**b**), respectively. Quantitative estimation of mitochondrial (**c**) and lysosomal (**d**) integrity in RAW 264.7 cells ($n = 5$–10/concentration). $^{**}P < 0.01$, $^{***}P < 0.001$ w.r.t. control determined by One-way ANOVA followed by Tukey's test

Therefore, when the two fluorophores are ~5.6 nm apart, the FRET efficiency will be reduced to one-half of the maximum. Imaging of CNT bundles was performed since individual CNTs can not be observed under confocal microscope. Physical mixing of fluorescein-labeled PF68 and RBITC-labeled CNTs showed poor FRET efficiency suggesting that PEO blocks are oriented away from the CNT surface. However, FRET efficiency was increased following phase inversion whereby the PPO blocks extend into the external non-aqueous medium and PEO blocks extend into the aqueous medium in the vicinity of CNTs. These results suggest that PPO blocks of PF68 tether to the CNT surface while the PEO blocks extend

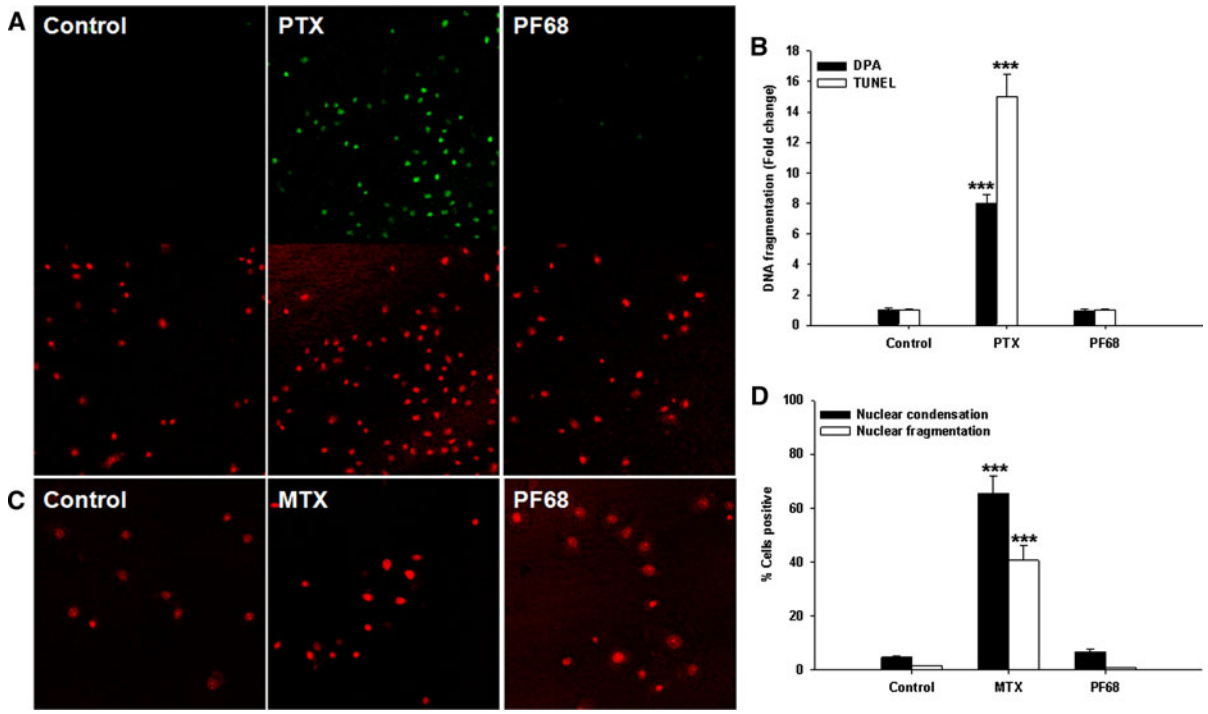

Fig. 9 DNA (**a**, **b**) and nuclear (**c**, **d**) integrity of RAW 264.7 cells incubated with medium alone (control), positive control, or PF68. The *upper panel* in (**a**) shows TUNEL-positive cells and *lower panel* shows nuclei counterstained with PI (200–300 cells were counted per concentration; $n = 5$–10/concentration). $^{***}P < 0.001$ w.r.t. control determined by One-way ANOVA followed by Tukey's test

into the aqueous medium and forms the corona. The FRET results were further confirmed by ^{1}H NMR. The PF68 concentration used in biocompatibility and FRET studies (0.3 %) was too low to be applicable in NMR spectroscopy. Therefore, 1 % PF68 was used in NMR spectroscopy. We believe that an increase in PF68 concentration would not influence the mechanism of CNT–PF68 interactions since both the concentrations used (0.3 and 1 %) were below critical micellization concentration. The preferential changes in ^{1}H NMR spectrum (peak shape, width, and chemical shifts) of PO blocks as compared to EO blocks suggest that PF68 binds to CNTs via the PO blocks whereby PO blocks form the hydrophobic core (Fig. 11). Therefore, NMR studies supported the observations in FRET studies. Similar results have also been demonstrated during micellization of pluronics (Ma et al. 2007). Our results are in agreement with earlier studies demonstrating that triblock block polymers, like pluronics, stabilize CNTs by a non-wrapping mechanism. The PPO block attaches to the CNT surface while the PEO blocks are tethered to the CNT through the PPO block. This leads to the formation of a steric barrier that prevents CNTs from aggregating. Since the mechanism of stabilization involves a "non-wrapping" mechanism, the electronic structure of the CNT remains unchanged (Nativ-Roth et al. 2007). Similar results have been demonstrated by small angle neutron scattering (Granite et al. 2011), spin probe electron paramagnetic resonance (Florent et al. 2008), UV–Vis and Raman spectroscopy (Nativ-Roth et al. 2007), and molecular dynamics simulations (Nativ-Roth et al. 2007). It has been shown that pluronics are tightly bound to CNTs and Pluronic-dispersed CNTs form a stable suspended even after dilution to concentrations much below the critical concentration required to achieve stable dispersion (Nativ-Roth et al. 2007). Contrastingly, we observed that CNT-bound PF68 can be displaced by PF68 demonstrating that PF68 binding to CNTs is reversible in nature. Further, CNT-bound PF68 can be displaced by albumin and serum proteins (when added to culture medium). Pluronic displacement by serum proteins has been demonstrated in CNTs (Cherukuri et al.

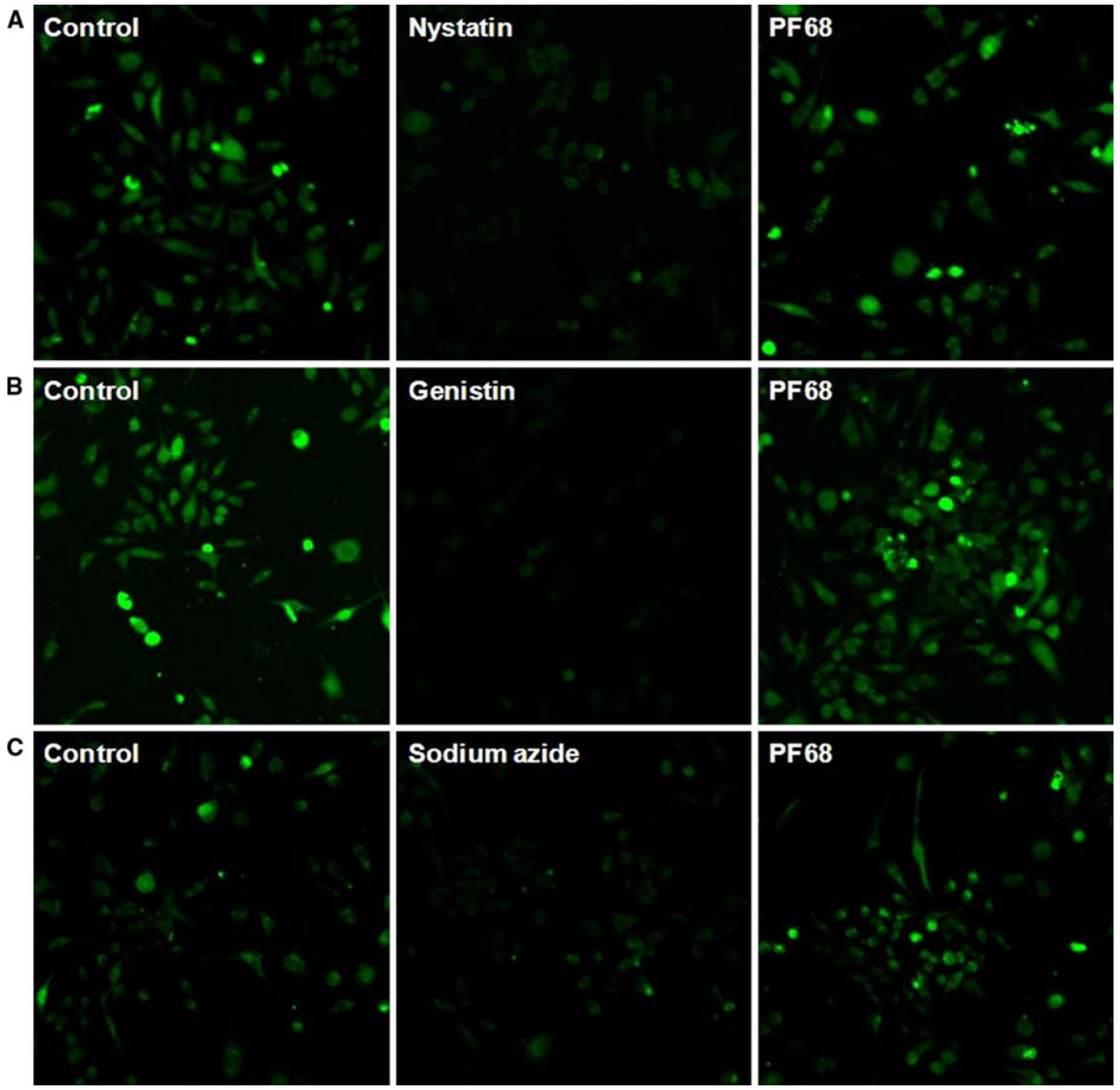

Fig. 10 Cellular uptake of caveolin (**a**), clathrin (**b**), and fluid phase (**c**) markers by RAW 264.7 cells incubated with marker alone (control; *first column*), marker + pathway-specific inhibitor (*middle panel*) or marker + PF68

2006) and nanospheres (Neal et al. 1998) as well. However, despite the displacement of PF68, CNT suspensions were stable in culture medium for 3 days. Significantly large amount of CNTs was retained in wells containing PF68-dispersed CNTs as compared to PBS-dispersed CNTs indicating that PF68-dispersed CNTs interact strongly with cells. A probable reason for higher degree of retention of PF68-dispersed CNTs following washing may be due to better dispersion of CNTs. Since the surfactant-free CNTs formed aggregates and floating clumps, the CNTs could not come into contact with cells. This leads to lesser degree of interaction between CNTs and cells. Hence, lesser amount of surfactant-free CNTs is retained. On the other hand, PF68-dispersed CNTs are uniformly dispersed in the culture medium, which leads to efficient CNT–cell interactions. Hence, PF68-dispersed CNTs are retained to a higher extent. The higher retention of PF68-dispersed CNTs was also associated with higher cellular uptake of CNTs.

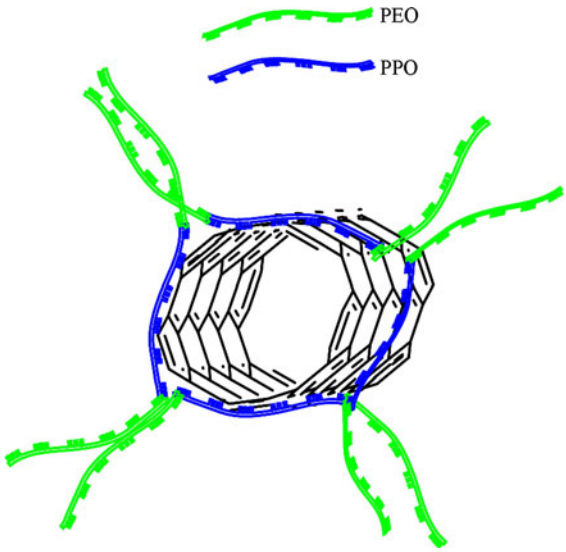

Fig. 11 Mechanism of CNT–PF68 interactions in aqueous medium. The hydrophobic PO blocks (*blue* color) tether to CNT surface while the hydrophilic EO blocks (*green* colored) extend in the aqueous medium. (Color figure online)

The displacement of PF68 by serum proteins raises the possibility that free PF68 can interact with cells and interfere with cellular functions. Such interference(s) may, possibility, influence the outcome of biocompatibility/toxicity studies. Thus, the effect of free PF68 on cellular functions was evaluated. Cell viability studies showed that 0.3 % PF68 was the highest permissible concentration that can be tolerated by a large variety of cell types. Further, the CNT suspensions were stable at 0.3 % PF68 concentration for up to 1 month. Hence, 0.3 % PF68 was selected for evaluation of effects on various biological functions. The addition and/or degradation of PF68 in culture medium can alter the physical properties of culture medium. These alterations may manifest as changes in pH and osmolarity of culture medium. We observed that PF68 did not alter these physical parameters during 3 days of incubation which further supported the use of PF68.

The absence of cell death does not qualify the biocompatibility of NPs since NPs may generate a stress response without inducing cell death (Pulskamp et al. 2007). Such a stress response may, at least theoretically, favor the toxic effects of NPs. Therefore, the effect of 0.3 % PF68 was evaluated on various possible targets of NP toxicity and included gross cell morphology, apoptosis, cell membrane, mitochondria, lysosomes, DNA, and nucleus. Flow cytometric analysis revealed that PF68 did not alter cell size or cellular complexity. Similarly, annexin V staining also revealed that PF68 did not induce apoptosis.

Several studies have highlighted the role of free radicals in NP toxicity and inflammation (Warheit et al. 2009). This is an important consideration in selection of surfactant for NPs as a pro-oxidant surfactant can enhance NP-stimulated generation of ROS leading to augmented or false-positive NP toxicity results. On the other hand, the use of natural surfactants for dispersion of CNTs (Porter et al. 2008) can interfere with activation of immunocytes and, thus, attenuate the inflammatory response (Raychaudhuri et al. 2004). Towards this end, we evaluated the effect of PF68 on stimulation of free radical (ROS and RNS) and cytokine production in macrophages and observed that PF68 showed no effect on free radical generation and cytokine production in macrophages.

NPs have been demonstrated to damage various cellular organelles like mitochondria (Teodoro et al. 2011; Wang et al. 2011), lysosomes (Zhong et al. 2010), and nucleus (Sriram et al. 2010; Srivastava et al. 2011). In addition, NPs may also influence the integrity of cell membrane (Hirano et al. 2008) and DNA (Guo et al. 2011; Xing et al. 2011). Mitochondrial and lysosomal damage are early events in cell death and lead to activation of cell death pathways (Terman et al. 2010). Similarly, alterations in nuclear morphology also indicate induction of cell death (Sriram et al. 2010; Srivastava et al. 2011). Further, nuclear fragmentation and DNA damage suggest genotoxic potential of NPs and can be considered as indicators of carcinogenicity (Norppa et al. 2011). NPs can also alter the integrity of cell membrane either directly or through activation of other effector molecules (Chen et al. 2009; de Planque et al. 2011; Ruenraroengsak et al. 2013). Therefore, the ability of PF68 to alter the integrity of these cellular components can influence the toxicity profile of NPs. However, experimental studies in the present report suggest that PF68 does not affect the integrity of cell organelles, cell membrane, or DNA suggesting the suitability of PF68 as a NP stabilizing agent.

The absence of adverse effect of PF68 on cellular physiology supports the applicability of PF68 as a biocompatible stabilizing agent for NP suspensions intended for biomedical applications as well as nanotoxicological screening. The higher biological

activity of NPs as compared to corresponding bulk materials is conferred by their small size which leads to higher cellular uptake via caveolin- and clathrin-mediated pathways and fluid phase uptake (Buono et al. 2009; Harush-Frenkel et al. 2008; Nam et al. 2009; Xu et al. 2010). Interference of PF68 with these pathways can alter the cellular uptake and biological profile of NPs. By applying fluorescent markers of caveolin (BSA) (Shajahan et al. 2004), clathrin (insulin) (Bacic et al. 2006), and fluid phase transfer (dextran) (Bacic et al. 2006), we observed that PF68 did not affect the cellular uptake of marker molecules. Therefore, the apparent absence of interference of PF68 with cellular uptake mechanisms along with its biocompatibility makes PF68 an ideal molecule for stabilization of NP dispersions.

The results of the present study suggest that unbound PF68, existing as free molecules in culture medium, did not induce cell death. Further, PF68 did not induce early signs of apoptotic or necrotic cell death since cell morphology, annexin V staining, and organelle integrity remained unaltered. In addition, PF68 showed no effect on cellular uptake mechanisms suggesting that PF68 has no influence on uptake of nutrients and other molecules by cells. These results suggest good biocompatibility of PF68.

In conclusion, the applicability of PF68 as an efficient, biocompatible NP stabilizing agent was investigated using CNTs as model NPs. The use of PF68 offers two major advantages. First, the NP suspensions formulated using PF68 are stable for a long duration. The ability to autoclave the CNT suspension, without affecting its size distribution, is important since terminal sterilization procedures insure sterility of the formulation and are convenient to perform on a commercial scale. The thermostability of CNT suspensions may be attributed to the high cloud point of PF68 (>100 °C). Further, the heating step (autoclaving in the present study) can also help in better dispersion of CNTs (Ciofani et al. 2009). Second, PF68 is biocompatible in in vitro and in vivo systems (Batrakova and Kabanov 2008; Kabanov and Alakhov 2002) and does not interfere with normal cellular physiological functions. This is evident from the absence of adverse effects on cell viability as well as cell membrane, mitochondrial, and lysosomal integrity. Further, PF68 neither induced stress responses nor interfered with cellular uptake pathways at the concentration tested. Thus, PF68-stabilized NP formulations can be conveniently adopted for pharmaceuticals intended for human use as well as for experimental in vitro and in vivo studies.

Acknowledgments The work was funded by grants from the Department of Science and Technology (DST) and Department of Pharmaceuticals, Ministry of Chemicals and Fertilizers, Government of India. The authors would like to thank Mr. Dinesh Chauhan for SEM studies and the Central Instrumentation Laboratory, NIPER for NMR studies. The authors also thank Mrs. Bhupinder Kaur and Department of Anatomy, PGIMER, Chandigarh for flow cytometry. RPS acknowledges DST for awarding Senior Research Fellowship.

Conflict of interest The authors declare no conflict of interest.

References

Antaris AL, Seo JW, Green AA, Hersam MC (2010) Sorting single-walled carbon nanotubes by electronic type using nonionic, biocompatible block copolymers. ACS Nano 4:4725–4732

Asati A, Santra S, Kaittanis C, Perez J (2010) Surface-charge-dependent cell localization and cytotoxicity of cerium oxide nanoparticles. ACS Nano 4:5321–5331

Bacic D, LeHir M, Biber J, Kaissling B, Murer H, Wagner CA (2006) The renal Na+/phosphate cotransporter NaPi-IIa is internalized via the receptor-mediated endocytic route in response to parathyroid hormone. Kidney Int 69:495–503

Batrakova EV, Kabanov AV (2008) Pluronic block copolymers: evolution of drug delivery concept from inert nanocarriers to biological response modifiers. J Control Release 130:98–106

Bihari P, Vippola M, Schultes S, Praetner M, Khandoga AG, Reichel CA, Coester C, Tuomi T, Rehberg M, Krombach F (2008) Optimized dispersion of nanoparticles for biological in vitro and in vivo studies. Part Fibre Toxicol 5:14

Blanch AJ, Lenehan CE, Quinton JS (2010) Optimizing surfactant concentrations for dispersion of single-walled carbon nanotubes in aqueous solution. J Phys Chem B 114:9805–9811

Buono C, Anzinger JJ, Amar M, Kruth HS (2009) Fluorescent pegylated nanoparticles demonstrate fluid-phase pinocytosis by macrophages in mouse atherosclerotic lesions. J Clin Invest 119:1373–1381

Chen J, Hessler JA, Putchakayala K, Panama BK, Khan DP, Hong S, Mullen DG, DiMaggio SC, Som A, Tew GN, Lopatin AN, Baker JR, Holl MMB, Orr BG (2009) Cationic nanoparticles induce nanoscale disruption in living cell plasma membranes. J Phys Chem B 113:11179–11185

Cherukuri P, Gannon CJ, Leeuw TK, Schmidt HK, Smalley RE, Curley SA, Weisman RB (2006) Mammalian pharmacokinetics of carbon nanotubes using intrinsic near-infrared fluorescence. Proc Natl Acad Sci 103:18882–18886

Ciofani G, Raffa V, Pensabene V, Menciassi A, Dario P (2009) Dispersion of multi-walled carbon nanotubes in aqueous pluronic F127 solutions for biological applications. Fuller Nanotub Car N 17:11–25

Crouzier T, Nimmagadda A, Nollert MU, McFetridge PS (2008) Modification of single walled carbon nanotube surface chemistry to improve aqueous solubility and enhance cellular interactions. Langmuir 24:13173–13181

de Planque MR, Aghdaei S, Roose T, Morgan H (2011) Electrophysiological characterization of membrane disruption by nanoparticles. ACS Nano 5:3599–3606

Dong L, Joseph KL, Witkowski CM, Craig MM (2008) Cytotoxicity of single-walled carbon nanotubes suspended in various surfactants. Nanotechnology 19:255702/255701–255702/255705

Duan WH, Wang Q, Collins F (2011) Dispersion of carbon nanotubes with SDS surfactants: a study from a binding energy perspective. Chem Sci 2:1407–1413

Elgrabli D, Abella-Gallart S, Aguerre-Chariol O, Robidel F, Rogerieux F, Boczkowski J, Lacroix G (2007) Effect of BSA on carbon nanotube dispersion for in vivo and in vitro studies. Nanotoxicology 1:266–278

Florent M, Shvartzman-Cohen R, Goldfarb D, Yerushalmi-Rozen R (2008) Self-assembly of pluronic block copolymers in aqueous dispersions of single-wall carbon nanotubes as observed by spin probe EPR. Langmuir 24:3773–3779

Gil PR, Oberdorster G, Elder A, Puntes V, Parak WJ (2010) Correlating physico-chemical with toxicological properties of nanoparticles: the present and the future. ACS Nano 4:5527–5531

Granite M, Radulescu A, Pyckhout-Hintzen W, Cohen Y (2011) Interactions between block copolymers and single-walled carbon nanotubes in aqueous solutions: a small-angle neutron scattering study. Langmuir 27:751–759

Guo YY, Zhang J, Zheng YF, Yang J, Zhu XQ (2011) Cytotoxic and genotoxic effects of multi-wall carbon nanotubes on human umbilical vein endothelial cells in vitro. Mutat Res 721:184–191

Harush-Frenkel O, Rozentur E, Benita S, Altschuler Y (2008) Surface charge of nanoparticles determines their endocytic and transcytotic pathway in polarized MDCK cells. Biomacromolecules 9:435–443

Hirano S, Kanno S, Furuyama A (2008) Multi-walled carbon nanotubes injure the plasma membrane of macrophages. Toxicol Appl Pharmacol 232:244–251

Inacio AS, Mesquita KA, Baptista M, Ramalho-Santos J, Vaz WLC, Vieira OV (2011) In vitro surfactant structure-toxicity relationships: implications for surfactant use in sexually transmitted infection prophylaxis and contraception. PLoS One 6:e19850

Jain AK, Swarnakar NK, Godugu C, Singh RP, Jain S (2011a) The effect of the oral administration of polymeric nanoparticles on the efficacy and toxicity of tamoxifen. Biomaterials 32:503–515

Jain AK, Swarnakar NK, Godugu C, Singh RP, Poduri RR, Jain S (2011b) Augmented anticancer efficacy of doxorubicin loaded polymeric nanoparticles after oral administration in breast cancer induced animal model. Mol Pharm 8:1140–1151

Kabanov AV, Alakhov VY (2002) Pluronic block copolymers in drug delivery: from micellar nanocontainers to biological response modifiers. Crit Rev Ther Drug Carrier Syst 19:1–73

Kawski A, Kuten E, Kaminski J (1973) Fluorescence quenching and nonradiative energy transfer in solutions. J Phys B 6:1907–1916

Lee JH, Hong SK, Kim JM, Ko WB (2011) Synthesis of gold nanoparticles using pluronic F127NF under microwave irradiation and catalytic effects. J Nanosci Nanotechnol 11:734–737

Ma J-H, Guo C, Tang Y-L, Liu H-Z (2007) 1H NMR spectroscopic investigations on the micellization and gelation of PEO–PPO–PEO block copolymers in aqueous solutions. Langmuir 23:9596–9605

Ma G, Yang J, Zhang L, Song C (2010) Effective antitumor activity of paclitaxel-loaded poly (epsilon-caprolactone)/pluronic F68 nanoparticles after intratumoral delivery into the murine breast cancer model. Anticancer Drugs 21:261–269

Meng H, Xia T, George S, Nel AE (2009) A predictive toxicological paradigm for the safety assessment of nanomaterials. ACS Nano 3:1620–1627

Nam HY, Kwon SM, Chung H, Lee SY, Kwon SH, Jeon H, Kim Y, Park JH, Kim J, Her S, Oh YK, Kwon IC, Kim K, Jeong SY (2009) Cellular uptake mechanism and intracellular fate of hydrophobically modified glycol chitosan nanoparticles. J Control Release 135:259–267

Nativ-Roth E, Shvartzman-Cohen R, Bounioux C, Florent M, Zhang D, Szleifer I, Yerushalmi-Rozen R (2007) Physical adsorption of block copolymers to SWNT and MWNT: a nonwrapping mechanism. Macromolecules 40:3676–3685

Neal JC, Stolnik S, Schacht E, Kenawy ER, Garnett MC, Davis SS, Illum L (1998) In vitro displacement by rat serum of adsorbed radiolabeled poloxamer and poloxamine copolymers from model and biodegradable nanospheres. J Pharm Sci 87:1242–1248

Norppa H, Catalan J, Falck G, Hannukainen K, Siivola K, Savolainen K (2011) Nano-specific genotoxic effects. J Biomed Nanotechnol 7:19

Porter D, Sriram K, Wolfarth M, Jefferson A, Schwegler-Berry D, Andrew M, Castranova V (2008) A biocompatible medium for nanoparticle dispersion. Nanotoxicology 2:144–154

Pulskamp K, Diabate S, Krug HF (2007) Carbon nanotubes show no sign of acute toxicity but induce intracellular reactive oxygen species in dependence on contaminants. Toxicol Lett 168:58–74

Raja PMV, Connolley J, Ganesan Gopal P, Ci L, Ajayan Pulickel M, Nalamasu O, Thompson Deanna M (2007) Impact of carbon nanotube exposure, dosage and aggregation on smooth muscle cells. Toxicol Lett 169:51–63

Rawat MK, Jain A, Singh S (2011) Studies on binary lipid matrix based solid lipid nanoparticles of repaglinide: in vitro and in vivo evaluation. J Pharm Sci 100:2366–2378

Raychaudhuri B, Abraham S, Bonfield TL, Malur A, Deb A, DiDonato JA, Kavuru MS, Thomassen MJ (2004) Surfactant blocks lipopolysaccharide signaling by inhibiting both mitogen-activated protein and IkappaB kinases in human alveolar macrophages. Am J Respir Cell Mol Biol 30:228–232

Ruenraroengsak P, Novak P, Berhanu D, Thorley AJ, Valsami-Jones E, Gorelik J, Korchev YE, Tetley TD (2013) Respiratory epithelial cytotoxicity and membrane damage (holes) caused by amine-modified nanoparticles. Nanotoxicology 6:94–108

Shajahan AN, Timblin BK, Sandoval R, Tiruppathi C, Malik AB, Minshall RD (2004) Role of Src-induced dynamin-2

phosphorylation in caveolae-mediated endocytosis in endothelial cells. J Biol Chem 279:20392–20400

Singh RP, Ramarao P (2012) Cellular uptake, intracellular trafficking and cytotoxicity of silver nanoparticles. Toxicol Lett 213:249–259

Singh RP, Das M, Thakare V, Jain S (2012) Functionalization density dependent toxicity of oxidized multiwalled carbon nanotubes in a murine macrophage cell line. Chem Res Toxicol 25:2127–2137

Sriram MI, Kanth SB, Kalishwaralal K, Gurunathan S (2010) Antitumor activity of silver nanoparticles in Dalton's lymphoma ascites tumor model. Int J Nanomed 5:753–762

Srivastava RK, Pant AB, Kashyap MP, Kumar V, Lohani M, Jonas L, Rahman Q (2011) Multi-walled carbon nanotubes induce oxidative stress and apoptosis in human lung cancer cell line-A549. Nanotoxicology 5:195–207

Strupp W, Weidinger G, Scheller C, Ehret R, Ohnimus H, Girschick H, Tas P, Flory E, Heinkelein M, Jassoy C (2000) Treatment of cells with detergent activates caspases and induces apoptotic cell death. J Membr Biol 175:181–189

Teodoro JS, Simoes AM, Duarte FV, Rolo AP, Murdoch RC, Hussain SM, Palmeira CM (2011) Assessment of the toxicity of silver nanoparticles in vitro: a mitochondrial perspective. Toxicol In Vitro 25:664–670

Terman A, Kurz T, Navratil M, Arriaga EA, Brunk UT (2010) Mitochondrial turnover and aging of long-lived postmitotic cells: the mitochondrial-lysosomal axis theory of aging. Antioxid Redox Signal 12:503–535

Thakare V, Das M, Jain AK, Patil S, Jain S (2010) Carbon nanotubes in cancer theragnosis. Nanomedicine 5:1277–1301

Vankoningsloo S, Piret JP, Saout C, Noel F, Mejia J, Zouboulis CC, Delhalle J, Lucas S, Toussaint O (2010) Cytotoxicity of multi-walled carbon nanotubes in three skin cellular models: effects of sonication, dispersive agents and corneous layer of reconstructed epidermis. Nanotoxicology 4:84–97

Wang L, Liu Y, Li W, Jiang X, Ji Y, Wu X, Xu L, Qiu Y, Zhao K, Wei T, Li Y, Zhao Y, Chen C (2011) Selective targeting of gold nanorods at the mitochondria of cancer cells: implications for cancer therapy. Nano Lett 11:772–780

Warheit DB, Reed KL, Sayes CM (2009) A role for nanoparticle surface reactivity in facilitating pulmonary toxicity and development of a base set of hazard assays as a component of nanoparticle risk management. Inhal Toxicol 21:61–67

Wick P, Manser P, Limbach LK, Dettlaff-Weglikowska U, Krumeich F, Roth S, Stark WJ, Bruinink A (2007) The degree and kind of agglomeration affect carbon nanotube cytotoxicity. Toxicol Lett 168:121–131

Xing Y, Xiong W, Zhu L, Osawa E, Hussin S, Dai L (2011) DNA damage in embryonic stem cells caused by nanodiamonds. ACS Nano 5:2376–2384

Xu Y, Liu BR, Lee HJ, Shannon KB, Winiarz JG, Wang TC, Chiang HJ, Huang YW (2010) Nona-arginine facilitates delivery of quantum dots into cells via multiple pathways. J Biomed Biotechnol 2010:948543

Zhong Y, Yingge Z, Yanlian Y, Lan S, Dong H, Hong L, Chen W (2010) Pharmacological and toxicological target organelles and safe use of single-walled carbon nanotubes as drug carriers in treating Alzheimer disease. Nanomedicine 6:427–441